Eur. Phys. J. E (2015) **38**: 19
DOI 10.1140/epje/i2015-15019-2

THE EUROPEAN PHYSICAL JOURNAL E

Regular Article

Onset and nonlinear regimes of ternary mixture convection in a square cavity*

T. Lyubimova[a] and N. Zubova

Institute of Continuous Media Mechanics UB RAS, 614013, Perm, Russia

Received 16 July 2014 and Received in final form 15 December 2014
Published online: 26 March 2015 –

Abstract. We present the results of numerical simulations of onset and nonlinear regimes of a ternary mixture convection in a square cavity subjected to the gravity field and vertical gradients of temperature and concentration. The stability problem for the non-convective state of the mixture is solved using a software package for the investigation of the stability of flows. Nonlinear regimes of convection are studied numerically by the finite difference method. The dependences of critical parameters on the net separation ratio are obtained for the cases of heating from above and below. Numerical data on the temporal evolution of the integral characteristics of flow and heat and mass transfer and of the fields of stream function, temperature and concentration are obtained for different values of the Rayleigh number and net separation ratio.

1 Introduction

Convection in multicomponent systems, which include real liquids and gases, is a poorly studied area. This is due to the fact that in multicomponent mixtures mass transfer of any component can be caused not only by the concentration gradient of this component, but also by cross-diffusion and thermal diffusion, which greatly complicates the study of such mixtures behaviour. Convective phenomena play an important role in many natural and technological processes. In particular, the composition of hydrocarbon deposits depends on diffusion and thermal diffusion processes (in the presence of geothermal gradient). Thermal diffusion is used for separation of isotopes in liquid and gas mixtures as well as in other separation processes which include colloids, nanofluids or macromolecules.

Convective stability of a binary mixture consisting of a non-reactive component was considered in [1]. In chapt. 7 of this monograph monotonic and oscillatory instabilities are found in the case when heat and mass fluxes are different and independent of each other in equilibrium state. The review on instability of a plane horizontal layer of a binary mixture studied within the framework of linear, weakly nonlinear and nonlinear theories can be found in [2].

Numerical investigation of Soret-driven convection in a mixture of water and isopropanol with the mass fraction ratio 9 : 1 in a cubic cavity, heated from above, at various levels of gravity was carried out in [3]. The paper presents the data on the temporal evolution of vertical component of the velocity, temperature and concentration, as well as the dependence of time for the onset of convection on the solutal Rayleigh number. For the linear stability problem of the Soret-driven binary mixture convection in a horizontal layer heated from above, the dependence of time for the onset of convection on the solutal Rayleigh number is obtained in [4]. In [5–8] a Soret-driven convection in colloidal suspensions was studied theoretically and experimentally. It was found that both the time needed to trigger the instability and the period of the observed oscillations obey power law behaviour as a function of the solutal Rayleigh number. Inclined layer convection was studied experimentally in [9] for a binary liquid mixture and in [10] for a colloidal suspension with negative Soret coefficient at large solutal Rayleigh numbers. The results on the stability of mechanical equilibrium in binary and ternary mixtures with the Soret effect in a plane horizontal layer with rigid and free boundaries are presented in [11]. The stability of equilibrium in a ternary mixture layer has been studied in [12]. Linear stability analysis of a horizontal layer of water-isopropanol-ethanol ternary mixture, heated from above, was performed in [13] neglecting cross effects.

In order to describe and predict heat and mass transfer in multicomponent mixtures, it is necessary to know the diffusion and thermal diffusion coefficients. In [14] the authors describe the technique for measuring the coefficients of thermal diffusion by digital optical interferometry and present the results of the application of this technique to

* Contribution to the Topical Issue "Thermal non-equilibrium phenomena in multi-component fluids" edited by Fabrizio Croccolo and Henri Bataller.

[a] e-mail: lubimova@psu.ru

the binary mixture of water and isopropanol. In [15] the thermal diffusion coefficients for hydrocarbon binary mixtures were measured by the thermogravitational column technique varying the molecular weight of alkanes in the mixture; the density dependence on temperature and concentration is obtained.

In [16] analytical and numerical stability analysis of the Soret-driven convection in a 2D porous cavity saturated by a binary fluid was carried out. The authors obtained the stability diagram, isoconcentrations, isotherms, and streamlines in the case of realistic boundary conditions. In [17] non-equilibrium diffusive processes in binary liquid mixtures were studied in the framework of the fluctuating hydrodynamics approach with consideration of the cases of mass diffusion, thermal diffusion, and pressure diffusion. The pressure diffusion effect was studied experimentally in [18], where Moiré deflectometry technique is applied to the investigation of diffusion dynamics of sugar in pure water.

The density dependences on temperature and concentrations and the concentration fields are obtained in [19] for the ternary hydrocarbon mixture in a two-dimensional cavity filled with a porous medium, subjected to the combined heating, accounting effects of thermal diffusion and barodiffusion, for different permeabilities of the medium.

The influence of static gravity level on the Soret-driven convection of a ternary mixture with the components having different signs of the separation ratio in a square cavity heated from above is investigated numerically in [20].

In [21] the long-wave instability of a multicomponent mixture steady flow in a vertical layer whose boundaries are maintained at different temperatures was studied. The problem was solved excluding cross-diffusion effects.

In practice, we often have to deal with a closed cavity. Therefore it is necessary to define the boundaries of stability of the multicomponent mixture in such geometry. This paper presents the results of a study of the onset and the nonlinear regimes of ternary mixture convection in a square cavity, conducted in preparation for the space experiment on measuring the diffusion and thermal diffusion coefficients. For pure thermal convection in a cubic cavity, it is found in [22] that the most dangerous perturbation "is similar to the one obtained for the two-dimensional case and appears as a roll where the hot liquid rises along one vertical wall and the cold liquid descends along the opposite wall". It justifies the use of 2D approach in our case.

2 Problem statement

Let us consider Soret-driven convection in a square cavity with the side L filled with a homogeneous multicomponent fluid. It is assumed that the cavity has rigid impermeable boundaries. The vertical boundaries are perfectly insulated and the horizontal boundaries are kept at constant different temperatures. The mixture density is a linear function of temperature T and concentration of components $\boldsymbol{C} = (C_1, \ldots, C_{n-1})^T$

$$\rho = \rho_0(1 - \beta_T(T - T_0) - \boldsymbol{I} \cdot \mathbf{B}(\boldsymbol{C} - \boldsymbol{C}_0)), \qquad (1)$$

where ρ_0, $\boldsymbol{C}_0 = (C_{1\,0}, \ldots, C_{n-1\,0})^T$ and T_0 are the initial density, the vector of concentrations and the temperature of the mixture, $\beta_T = -(1/\rho_0)(\partial\rho/\partial T)|_{C_i}$, $i = 1, \ldots, n-1$, is the thermal expansion coefficient, $\mathbf{B} = \mathrm{diag}\{\beta_{C_1}, \ldots, \beta_{C_{n-1}}\}$ is the diagonal matrix of solutal expansion coefficients (so $\beta_{C_i} = -(1/\rho_0)(\partial\rho/\partial C_i)|_{T,C_j}, j = 1, \ldots, n-1$, $i = 1, \ldots, n-1$, $j \neq i$), $\boldsymbol{I} = (1, \ldots, 1)$ is the unit vector.

To describe the free Soret-driven convection we use the following dimensionless unsteady equations in the Boussinesq approximation:

$$\frac{\partial \boldsymbol{u}}{\partial t} + (\boldsymbol{u} \cdot \nabla)\,\boldsymbol{u} = -\nabla p + \nabla^2 \boldsymbol{u} + \frac{\mathrm{Ra}}{\mathrm{Pr}}\,(T + \boldsymbol{I} \cdot \boldsymbol{C})\,\boldsymbol{k}, \qquad (2)$$

$$\frac{\partial T}{\partial t} + (\boldsymbol{u} \cdot \nabla)\,T = \mathrm{Pr}^{-1}\nabla^2 T, \qquad (3)$$

$$\frac{\partial \boldsymbol{C}}{\partial t} + (\boldsymbol{u} \cdot \nabla)\,\boldsymbol{C} = \mathbf{SC}\left(\nabla^2 \boldsymbol{C} - \boldsymbol{\psi}\nabla^2 T\right), \qquad (4)$$

$$\nabla \cdot \boldsymbol{u} = 0. \qquad (5)$$

Here $\boldsymbol{u}$ is the velocity vector, p is the pressure, $\boldsymbol{k}$ is the unit vertical vector. We introduce the following scaling quantities: L for the length, ν/L for the velocity, L^2/ν for the time, $\rho_0\nu^2/L^2$ for the pressure, the characteristic temperature difference ΔT is used for the temperature and $\beta_T \Delta T \mathbf{B}^{-1}$ for the vector of concentrations, where ν is the viscosity of the mixture. Equations (2)–(5) contain the following dimensionless parameters: $\boldsymbol{\psi} = -\beta_T^{-1}\mathbf{B}\mathbf{D}^{-1}\boldsymbol{D}_T$ is the vector of separation ratios having the dimension $(n-1)$, where $\mathbf{D}$ is the matrix of molecular diffusion coefficients, $\boldsymbol{D}_T$ is the vector of thermal diffusion coefficients, $\mathrm{Pr} = \nu/\alpha$ is the Prandtl number, where α is the thermal diffusivity, $\mathrm{Ra} = g\beta_T \Delta T L^3/(\nu\alpha)$ is the Rayleigh number, where g is the acceleration of gravity, $\mathbf{SC} = \nu^{-1}\mathbf{B}\mathbf{D}\mathbf{B}^{-1}$ is the matrix of parameters of the dimension $(n-1)\times(n-1)$, $\{\mathbf{SC}\}_{ij} = (\beta_{C_i}/\beta_{C_j})\mathrm{Sc}_{ij}^{-1}$, where $i, j = 1, \ldots, n-1$, $\mathrm{Sc}_{ii} = \nu/D_{ii}$ are Schmidt numbers, D_{ii} are diagonal elements of the diffusion matrix.

Generally, the concentration equation contains a pressure diffusion term. However, for hydrocarbons mixtures the pressure diffusion coefficient, as well as the ratio of pressure diffusion term to thermal diffusion term are small. For example, for gaseous mixture of methane, ethane, iso-butane the pressure diffusion coefficient is of the order of 10^{-16}, and the ratio of two terms mentioned above $\sim 10^{-10}$ [19]. For this reason, in the present paper the effect of pressure diffusion is not considered.

By diagonalizing matrix of molecular diffusion coefficients in the initial dimensional equations, we can eliminate the cross-diffusion effects, which reduces the number of governing parameters. This transformation in dimensionless form can be written as [21]

$$\boldsymbol{C} = \mathbf{B}\mathbf{V}(\mathbf{B}\mathbf{Q})^{-1}\hat{\boldsymbol{C}}, \qquad \boldsymbol{\psi} = \mathbf{B}\mathbf{V}(\mathbf{B}\mathbf{Q})^{-1}\hat{\boldsymbol{\psi}}, \qquad (6)$$

where $\mathbf{V}$ is the matrix whose columns are the eigenvectors $v_i = (v_{i1}, \ldots, v_{in-1})^T$ of the matrix $\mathbf{D}$, $\mathbf{Q}$ is the diagonal matrix, $q_i = \beta_i^{-1}\sum_{j=1}^{n-1}\beta_j v_{ij}$.

The transformation (6) allows to reduce the dimensionless equations to a system with a diagonal matrix

$\hat{\mathbf{SC}} = \nu^{-1}\hat{\mathbf{D}}$, vector of concentration $\hat{\boldsymbol{C}}$ and vector of separation ratios $\hat{\boldsymbol{\psi}}$.

$$\frac{\partial \boldsymbol{u}}{\partial t} + (\boldsymbol{u}\cdot\nabla)\,\boldsymbol{u} = -\nabla p + \nabla^2\boldsymbol{u} + \frac{\mathrm{Ra}}{\mathrm{Pr}}\left(T + \boldsymbol{I}\cdot\hat{\boldsymbol{C}}\right)\boldsymbol{k}, \quad (7)$$

$$\frac{\partial T}{\partial t} + (\boldsymbol{u}\cdot\nabla)\,T = \mathrm{Pr}^{-1}\nabla^2 T, \quad (8)$$

$$\frac{\partial \hat{\boldsymbol{C}}}{\partial t} + (\boldsymbol{u}\cdot\nabla)\,\hat{\boldsymbol{C}} = \hat{\mathbf{SC}}\left(\nabla^2\hat{\boldsymbol{C}} - \hat{\boldsymbol{\psi}}\nabla^2 T\right), \quad (9)$$

$$\nabla\cdot\boldsymbol{u} = 0. \quad (10)$$

At the boundaries we impose the no-slip conditions, the absence of diffusion flux of solutes, fixed different temperatures at the horizontal boundaries and the absence of heat flux at vertical boundaries:

$$x = 0,1:\ \boldsymbol{u} = 0, \qquad \frac{\partial T}{\partial x} = \frac{\partial \hat{\boldsymbol{C}}}{\partial x} = 0, \quad (11)$$

$$y = 0,1:\ \boldsymbol{u} = 0,\ T = \pm 1/2, \qquad \frac{\partial \hat{\boldsymbol{C}}}{\partial y} - \hat{\boldsymbol{\psi}}\frac{\partial T}{\partial y} = 0. \quad (12)$$

3 Linear stability problem

The problem (7)–(12) allows the solution, corresponding to the mechanical equilibrium:

$$\boldsymbol{u}_s = 0, \qquad p_s = \frac{\mathrm{Ra}(\Psi+1)}{2\,\mathrm{Pr}}(y - y^2),$$
$$T_s = \frac{1}{2} - y, \qquad \hat{\boldsymbol{C}}_s = \Psi\left(\frac{1}{2} - y\right), \quad (13)$$

where $\Psi = \psi_1 + \ldots + \psi_{n-1}$ is the net separation ratio. The case $\mathrm{Ra} > 0$ corresponds to the heating from below and $\mathrm{Ra} < 0$ – to the heating from above.

Let us consider the stability of state (13) with respect to small perturbations. For that we represent the fields of velocity, temperature, pressure and concentrations as the sums of the base state (13) and small perturbations:

$$\left(\boldsymbol{u}, p, T, \hat{\boldsymbol{C}}\right) = \left(\boldsymbol{u}_s, p_s, T_s, \hat{\boldsymbol{C}}_s\right) + \left(\boldsymbol{u}', p', T', \hat{\boldsymbol{C}}'\right). \quad (14)$$

The linearized equations for small perturbations of the base state (13) have the form

$$\frac{\partial \boldsymbol{u}'}{\partial t} = -\nabla p' + \nabla^2\boldsymbol{u}' + \frac{\mathrm{Ra}}{\mathrm{Pr}}\left(T' + \boldsymbol{I}\cdot\hat{\boldsymbol{C}}'\right)\boldsymbol{k}, \quad (15)$$

$$\frac{\partial T'}{\partial t} + (\boldsymbol{u}'\cdot\nabla)\,T_s = \mathrm{Pr}^{-1}\nabla^2 T', \quad (16)$$

$$\frac{\partial \hat{\boldsymbol{C}}'}{\partial t} + (\boldsymbol{u}'\cdot\nabla)\,\hat{\boldsymbol{C}}_s = \hat{\mathbf{SC}}\left(\nabla^2\hat{\boldsymbol{C}}' - \hat{\boldsymbol{\psi}}\nabla^2 T'\right), \quad (17)$$

$$\nabla\cdot\boldsymbol{u}' = 0. \quad (18)$$

We restrict ourselves to the consideration of 2D perturbations and introduce stream function and vorticity as $\boldsymbol{u}'_x = \frac{\partial\psi}{\partial y}$, $\boldsymbol{u}'_y = -\frac{\partial\psi}{\partial x}$, $\varphi = \mathrm{curl}_z\,\boldsymbol{u} = -\Delta\psi$. Equations for small two-dimensional perturbations written in terms of the stream function and vorticity are as follows:

$$\frac{\partial\varphi}{\partial t} = \Delta\varphi + \mathrm{Ra}\ \mathrm{Pr}^{-1}\left(\frac{\partial T'}{\partial x} + \boldsymbol{I}\cdot\frac{\partial\hat{\boldsymbol{C}}'}{\partial x}\right), \quad (19)$$

$$\frac{\partial T'}{\partial t} - \frac{\partial\psi}{\partial x}\frac{\partial T_s}{\partial y} = \mathrm{Pr}^{-1}\Delta T', \quad (20)$$

$$\frac{\partial\hat{\boldsymbol{C}}'}{\partial t} - \frac{\partial\psi}{\partial x}\frac{\partial\hat{\boldsymbol{C}}_s}{\partial y} = \hat{\mathbf{SC}}\left(\Delta\hat{\boldsymbol{C}}' - \hat{\boldsymbol{\psi}}\Delta T'\right), \quad (21)$$

$$\varphi = -\Delta\psi. \quad (22)$$

The boundary conditions for the perturbations in terms of ψ and φ are

$$x = 0,1:\ \psi = \frac{\partial\psi}{\partial x} = \frac{\partial T'}{\partial x} = \frac{\partial\hat{\boldsymbol{C}}'}{\partial x} = 0, \quad (23)$$

$$y = 0,1:\ \psi = \frac{\partial\psi}{\partial x} = T' = \frac{\partial\hat{\boldsymbol{C}}'}{\partial y} - \hat{\boldsymbol{\psi}}\frac{\partial T'}{\partial y} = 0. \quad (24)$$

Let us consider the normal perturbations in the form $e^{-\lambda t}$, where $\lambda = \lambda_r + i\omega$ is the complex decrement, λ_r is the real part of decrement, ω is the circular frequency.

4 Numerical methods

The problem (19)–(24) was solved using a software package developed for the investigation of the stability of flows [23]. The generalized linear eigenvalue problem $\mathbf{A}\boldsymbol{x} = \lambda\mathbf{B}\boldsymbol{x}$, obtained by the discretization of the original problem by the finite difference method was solved. Here $\mathbf{A}$ is the sparse non-symmetric complex-valued matrix, $\mathbf{B}$ is a singular, diagonal matrix with either 0 or ± 1 at the diagonal, λ are the eigenvalues (decrements of perturbations), $\boldsymbol{x}$ is the eigenvector composed of the velocity perturbations (pressure, temperature, depending on the task). The original equations (19)–(22) with the boundary conditions (23), (24) were discretized on the mesh with uniform spatial step $h = 0.0256$. Spatial derivatives were approximated by finite differences of the second order.

To solve the spectral problem $\mathbf{A}\boldsymbol{x} = \lambda\mathbf{B}\boldsymbol{x}$ the Newton-Raphson method is used in the package [24].

The calculations of the linear stability problem were carried out for model ternary mixture with the following parameters: the Prandtl number $\mathrm{Pr} = 10$, Schmidt numbers $\mathrm{Sc}_1 = 100$, $\mathrm{Sc}_2 = 1000$ and the separation ratio of the first component $\psi_1 = 0.3$. These parameters are typical for liquid mixtures.

In addition to the solutions of linear stability problem, direct numerical simulation of nonlinear convection regimes for ternary mixture was conducted. Nonlinear equations (7)–(10) with the boundary conditions (11), (12), rewritten in terms of the stream function and vorticity, were solved numerically by finite difference method. Spatial derivatives were approximated by central differences. Unsteady equations were solved using explicit finite difference scheme with a constant time step $h^2/8$,

where h is spatial step. For nonlinear calculations we used the uniform spatial grid with the same step as that for the linear stability problem. This grid was chosen to ensure the optimum relation between the computation time and the required precision both in the linear and nonlinear cases. The Poisson equation for the stream function was solved by successive overrelaxation method. The vorticity values at the boundaries of the cavity were calculated using the Thom's formula [25]. The initial conditions corresponded to the mechanical equilibrium of the mixture. The algorithm and numerical code for the nonlinear calculations were tested by the problem of the Soret-driven convection of binary fluid.

5 The results for linear stability problem

In mixtures with the Soret effect the molecules of the component with negative separation ratio under the temperature gradient move to the warmer part of the cavity, and the molecules of the component with positive separation ratio to the colder part. If gravity is absent, convective flow in the mixture does not arise, there is only the thermal diffusion separation of components. In the presence of gravity, convective flow arises in the case when the heavier component of the mixture is situated above the lighter one.

For ternary fluid, if the ratio of the Schmidt numbers $\mathrm{Sc}_1/\mathrm{Sc}_2$ is small, then the diffusion properties of the second solute are significantly worse than that of the first solute, and the type of instability will be determined by the sign of the separation ratio ψ_2 of the second component. Because of that, we first discuss the case of binary mixture with the parameters equal to the parameters of the second solute of the ternary mixture. It is known [1] that for binary mixtures heated from above the concentration gradient of lighter component with positive Soret effect is directed towards the hot boundary, which leads to the stability of the system. For mixture with negative Soret effect the heavier component is accumulated near the hot boundary which leads to monotonic instability. Here, the sinking fluid element after the temperature equalization in the cavity to the temperature of the surrounding fluid will have greater density than that of the fluid, and will continue a downward motion.

In the case of heating from below the positive Soret effect leads to the decrease of critical Rayleigh number (hereinafter the critical Rayleigh number, $\mathrm{Ra_c}$), since the concentration gradient of the lighter component is directed towards the hot boundary. Since the density of the rising fluid element is always lower than that of the surrounding fluid, it will continue to rise despite of the mass diffusion and thermal conduction. Therefore, under the heating from below the monotonic instability is realized in binary mixtures with a positive separation ratio ψ_i.

The concentration gradient of the lighter component with negative Soret effect is directed towards the cold boundary, which leads to the increase of $\mathrm{Ra_c}$. The rising fluid element, as in the previous case, has lower density than the surrounding fluid, but after the cooling its density becomes higher than the density of the surrounding fluid and it moves to the bottom wall of the cavity. Thus, for negative values of the separation ratio less than a certain value ψ_*, the oscillatory perturbations are responsible for the equilibrium stability loss. In [1] to determine the value ψ_* for the problem of binary mixture convection in vertical layer with artificial boundary conditions (fixed concentrations at the boundaries) an expression is obtained, from which it follows that at $\mathrm{Sc} > \mathrm{Pr}$ the value ψ_* should be negative, and at $\mathrm{Sc} \gg \mathrm{Pr}$ it should be negative and close to zero. It was not possible to prove the monotonicity principle and to determine the range of oscillatory perturbations existence in the case of impermeable boundaries. The generalization of the monotonicity of perturbations for the case of a multicomponent mixture with the Soret effect for the same boundary conditions as in [1] was carried out in [11].

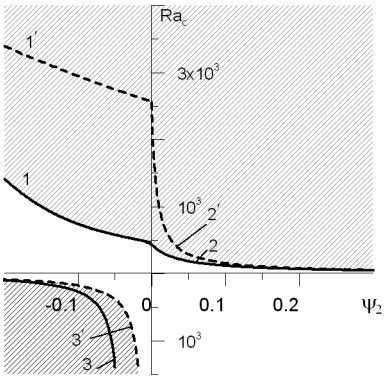

Fig. 1. Dependence of the critical Rayleigh number $\mathrm{Ra_c}$ on the separation ratio ψ_2. Solid lines: ternary mixture, dashed lines: binary mixture with $\mathrm{Pr} = 10$, $\mathrm{Sc}_2 = 1000$; curves 1 and $1'$: oscillatory instability boundaries; 2, $2'$ and 3, $3'$: monotonic instability boundaries; the domain of instability is shaded.

Our calculations for the case of binary mixture ($\psi_1 = 0$) at $\mathrm{Pr} = 10$, $\mathrm{Sc} = 1000$ (fig. 1, dashed lines), despite the use of other, more realistic conditions for the concentrations at the boundaries, give the results which well agree with [1]: the critical separation ratio Ψ_* approximately equals $-3 \cdot 10^{-5}$. The crosspoint of curve 2 with y-axis ($\psi_2 = 0, \Psi = 0$) corresponds to $\mathrm{Ra} \approx 2540$ which coincides with the value of Ra obtained in [1] for single-component fluid.

The results of our calculations for the ternary mixture with the above-indicated parameters are shown in fig. 1 (solid lines). As is described above, the type of instability is determined by the sign of the separation ratio ψ_2 of the second component, that is why the critical Rayleigh number is given in dependence on the separation ratio of the second component. It is seen that, as in the case of binary mixture, in ternary mixtures the oscillatory instability is observed under heating from below and the monotonic instability at heating from above and below. The point separating the domains of monotonic and oscillatory instabilities in this case is close to $\psi_2 \approx 0$. The calculations at Schmidt numbers $\mathrm{Sc}_1 = 100$ and $\mathrm{Sc}_2 = 1000$ gave for this point the value $\psi_2 \approx -0.003$ which is close to zero.

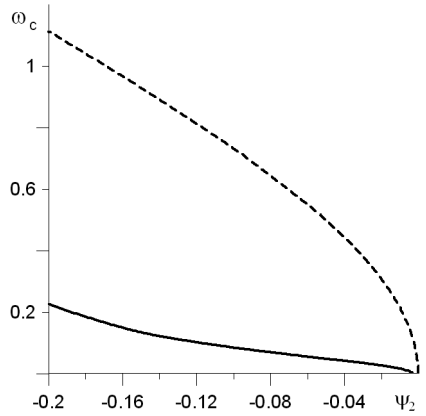

Fig. 2. Dependence of the critical circular frequency ω_c on separation ratio ψ_2. Solid line: ternary mixture, dashed line: binary mixture with $\mathrm{Pr} = 10$, $\mathrm{Sc}_2 = 1000$.

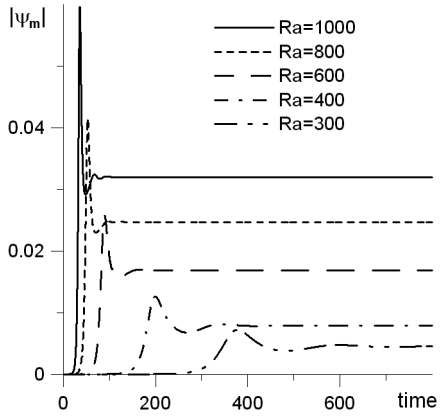

Fig. 3. Temporal evolution of $|\psi_m|$ for different Rayleigh number values. Mixture with $\psi_1 = 0.3$, $\psi_2 = 0.1$, $\Psi = \psi_1 + \psi_2 = 0.4$.

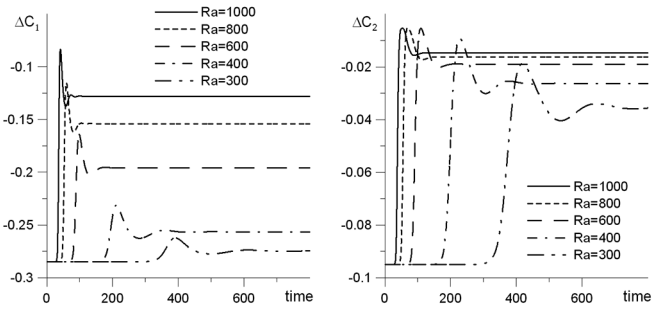

Fig. 4. Temporal evolution of the concentration difference between the centers of the upper and lower boundaries for the mixture with $\psi_1 = 0.3$, $\psi_2 = 0.1$, $\Psi = \psi_1 + \psi_2 = 0.4$.

Thus, in the case of ternary mixture heated from below ($\mathrm{Ra} > 0$) at $\psi_2 < -0.003$ the oscillatory perturbations are most dangerous and at $\psi_2 > -0.003$ the monotonic perturbations are the most dangerous.

The mixture with positive Soret effect of the second component is subjected to strong destabilizing effects of temperature and concentration gradients of both solutes. In the range of oscillatory instability the temperature gradient and the concentration gradient of the first solute destabilizes the system, and the concentration gradient of the second solute increases its stability. With $|\psi_2|$ growth in the domain $\Psi < 0.3$ the stabilizing influence of negative Soret effect of the second solute is also increasing, which is accompanied by the growth of the critical value of the Rayleigh number.

The monotonic perturbations are responsible for the instability at heating from above ($\mathrm{Ra} < 0$). The values $\Psi > 0.3$ correspond to the positive Soret effect of both solutes, and instability is not observed. When $\Psi < 0.3$, the first solute has a positive Soret effect (concentration gradient is stabilizing), and the second solute has negative Soret effect (concentration gradient plays a destabilizing role). This causes an instability of the mechanical equilibrium of mixture only under certain conditions. The dependence of the critical circular frequency on ψ_2 is shown in fig. 2. Note, that the critical frequency becomes zero at different values of the separation ratio for the binary and the ternary mixture.

As one can see from fig. 1, the addition of the solute with positive Soret effect ($\psi_1 = 0.3$) to the binary mixture leads to the destabilization of monotonic and oscillatory instabilities under heating from below and to the stabilization of the monotonic instability at heating from above. This is explained by the argument presented above for a binary mixture.

6 The results of nonlinear calculations

Let us illustrate the nonlinear regimes of the ternary mixture convection in a square cavity by an example of model mixtures with $\psi_1 = 0.3$, $\psi_2 = 0.1$, $\Psi = \psi_1 + \psi_2 = 0.4$ and $\psi_1 = 0.3$, $\psi_2 = -0.4$, $\Psi = \psi_1 + \psi_2 = -0.1$, heated from below, the mixture with $\psi_1 = 0.3$, $\psi_2 = -0.1$, $\Psi = \psi_1 + \psi_2 = 0.2$ heated from above, and the mixture dodecane-isobutylbenzene-tetralin, the components of which are taken in the proportions $1 : 1 : 1$.

For the mixture with $\psi_1 = 0.3$, $\psi_2 = 0.1$, $\Psi = \psi_1 + \psi_2 = 0.4$, heated from below, as shown in fig. 1, the monotonic instability is observed. Figures 3 and 4 show the time dependence of the characteristics of the convection: the module of maximum value of the stream function in the cavity (fig. 3) and the concentrations difference between the centers of the upper and lower boundaries (fig. 4) for different values of the Rayleigh number. During a certain period of time, the mixture remains in non-convective state (stream function is zero, fig. 3), then the fluctuations gradually increase and the flow arises. The concentration difference of the mixture component shows a similar behaviour (fig. 4). The onset of convection is accompanied by sharp jumps of the flow intensity and of the concentration difference between the upper and lower boundaries for both solutes. The lower the level of gravity, the later instability occurs, which later is replaced by steady flow.

The structure of the steady flows induced by the heating from below for a mixture with positive separation ra-

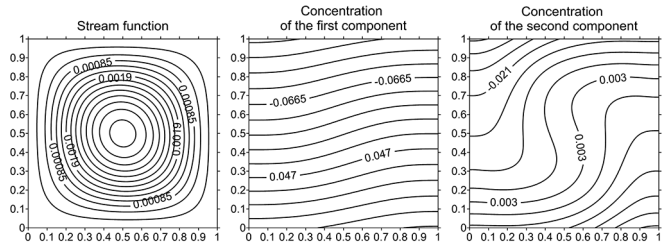

Fig. 5. Stream function and the component concentration fields for steady regimes of the mixture with $\psi_1 = 0.3$, $\psi_2 = 0.1$, $\Psi = \psi_1 + \psi_2 = 0.4$, Ra = 300.

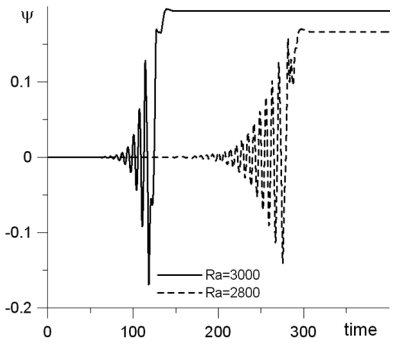

Fig. 6. Temporal evolution of the stream function in the center of the cavity for different Rayleigh number values. Mixture with $\psi_1 = 0.3$, $\psi_2 = -0.4$, $\Psi = \psi_1 + \psi_2 = -0.1$.

tios for both solutes for Ra = 300 is shown in fig. 5. The flow is single-vortex, the isolines of concentrations become deformed strongly with the increase of gravity. The solutes with positive separation ratios are accumulated near the hot lower boundary.

For the mixture with $\psi_1 = 0.3$, $\psi_2 = -0.4$, $\Psi = \psi_1 + \psi_2 = -0.1$, heated from above the oscillatory instability is observed, as is seen from fig. 1. The temporal evolution of the stream function in the center of the cavity is shown in fig. 6 for Ra = 2800, 3000. As seen, at the beginning the growing oscillations are observed, then they are replaced by the steady single vortex flow. Stream function, temperature and concentration fields are shown in fig. 7 for Ra = 3000. It is seen that the first solute with positive separation ratio $\psi_1 = 0.3$ is accumulated near the warm lower boundary and the second solute with negative separation ratio near the cold upper boundary.

The temporal evolution of the stream function in the center of cavity is shown in fig. 8 for Ra = 2646. This value of the Rayleigh number is close to the critical value $\mathrm{Ra_c} = 2645.5$ according to the linear stability results. We could see that at such low supercriticality the evolution time of perturbations is very larger. The frequency equals $\omega = 0.883$, while the critical value of frequency for the mixture with such parameters is $\omega_c = 0.88$. The transformation of the flow structure during the period of oscillations is shown in fig. 9 for Ra = 2646. Time moments for the corresponding flow structures are marked on the plot of the temporal evolution of the stream function in the center of the cavity (fig. 8b).

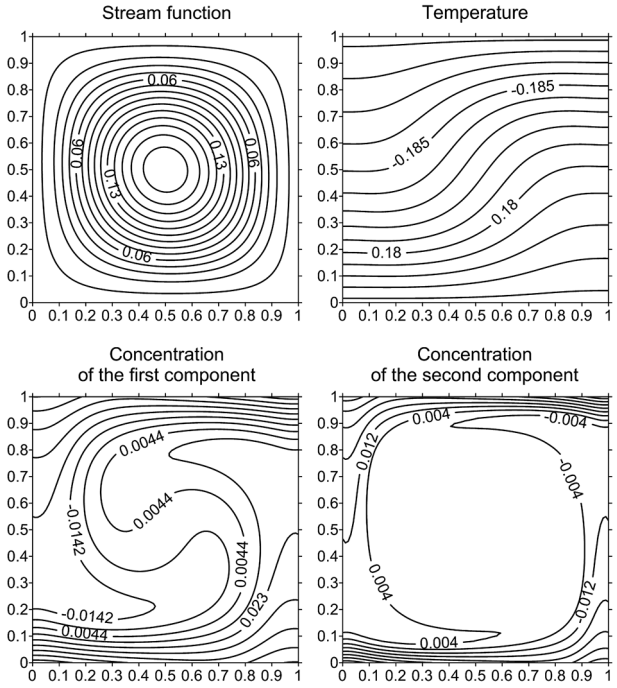

Fig. 7. Stream function, temperature and concentration fields for steady regimes of the mixture with $\psi_1 = 0.3$, $\psi_2 = -0.4$, $\Psi = \psi_1 + \psi_2 = -0.1$, Ra = 3000.

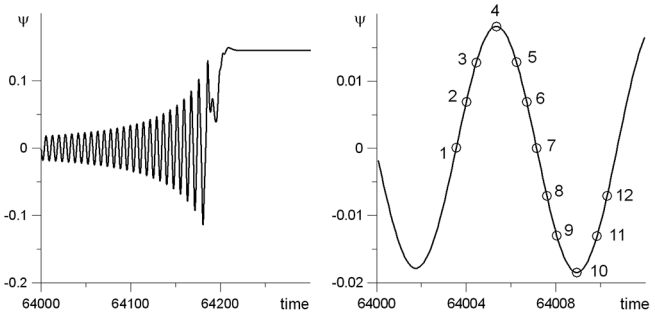

Fig. 8. (a) Temporal evolution of the stream function in the center of cavity. (b) Time moments for which the flow structures are presented. Mixture with $\psi_1 = 0.3$, $\psi_2 = -0.4$, $\Psi = \psi_1 + \psi_2 = -0.1$, Ra = 2646.

To illustrate the flow structure in the case of heating from above, we selected the mixture with $\psi_1 = 0.3$, $\psi_2 = -0.1$, $\Psi = \psi_1 + \psi_2 = 0.2$. As is seen from fig. 1, for this mixture the monotonic instability is observed. Temporal evolution of the modulus of maximal stream function and of the concentration difference between the centers of the upper and lower boundaries are presented in figs. 10, 11. The flow intensity increases monotonically until it reaches a constant value. The smaller the gravity the later the steady flow starts.

The steady flow is of single-vortex structure (fig. 12). The first solute with the separation ratio $\psi_1 = 0.3$ is accumulated near the warm upper boundary and the second solute with $\psi_2 = -0.1$ near the cold lower boundary. Parameters of the first solute correspond to non-convective

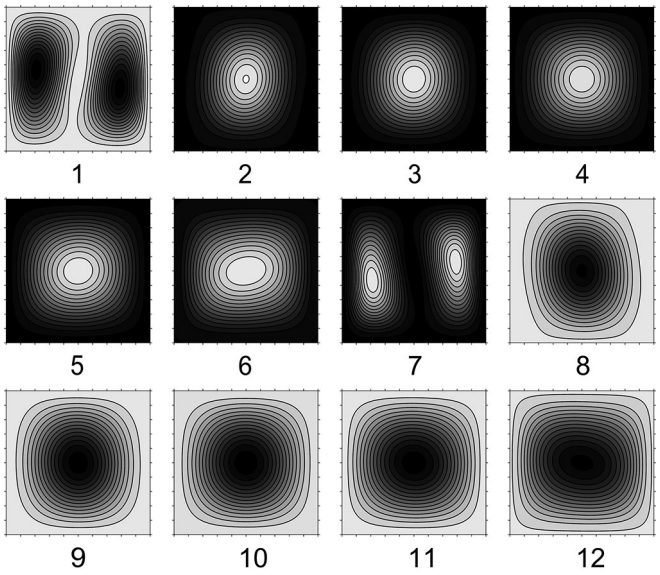

Fig. 9. Transformation of flow structure during the period of oscillations. Mixture with $\psi_1 = 0.3$, $\psi_2 = -0.4$, $\Psi = \psi_1 + \psi_2 = -0.1$, Ra = 2646. The white (black) color corresponds to the higher (lower) values of the stream function.

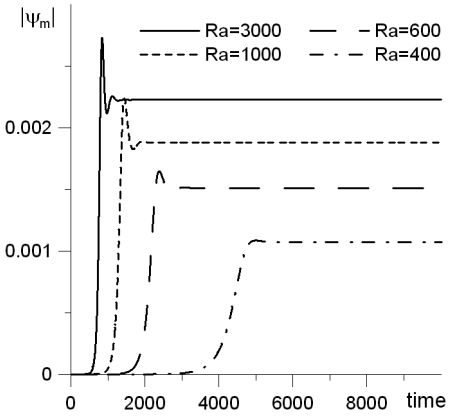

Fig. 10. Temporal evolution of $|\psi_m|$ for different Rayleigh number values. Mixture with $\psi_1 = 0.3$, $\psi_2 = -0.1$, $\Psi = \psi_1 + \psi_2 = 0.2$.

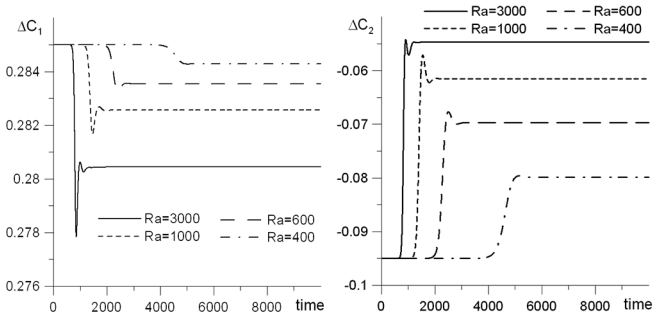

Fig. 11. Temporal evolution of the concentration difference between the centers of the upper and lower boundaries for the mixture with $\psi_1 = 0.3$, $\psi_2 = -0.1$, $\Psi = \psi_1 + \psi_2 = 0.2$.

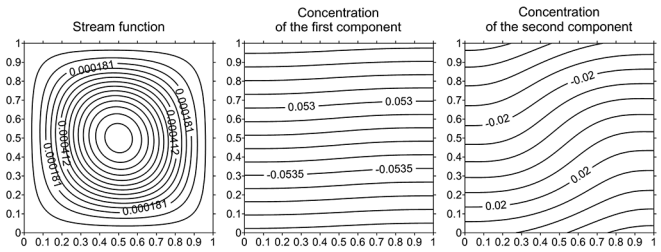

Fig. 12. Stream function and concentration fields for steady regimes of the mixture with $\psi_1 = 0.3$, $\psi_2 = -0.1$, $\Psi = \psi_1 + \psi_2 = 0.2$, Ra = 300.

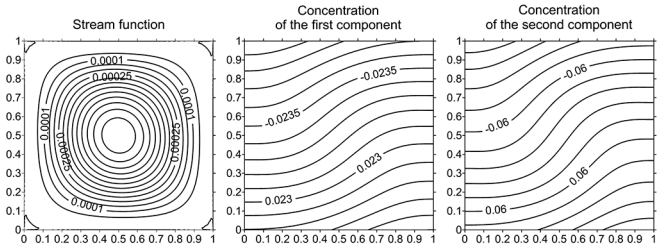

Fig. 13. Stream function and concentration fields for steady regimes of the mixture dodecane-isobutylbenzene-tetralin, Ra = 40.

case, but convection arises because of the destabilizing effect of the second solute with negative separation ratio. The concentration isolines of the first solute are weakly deformed. With the increase of Rayleigh number (level of gravity) the concentration field deformation becomes more pronounced.

The ternary mixture dodecane-isobutylbenzene-tetralin with components, taken in equal portions, at $T = 298\,\mathrm{K}$, has a thermal expansion coefficient $\beta_T = 0.914 \cdot 10^{-3} 1/\mathrm{K}$, solutal expansion coefficients $\beta_{C_1} = 0.258$, $\beta_{C_2} = 0.121$, kinematic viscosity $\nu = 1.528 \cdot 10^{-6}\,\mathrm{m}^2/\mathrm{s}$, mass diffusion coefficients $D_{11} = 6.70 \cdot 10^{-10}\,\mathrm{m}^2/\mathrm{s}$, $D_{12} = 0.43 \cdot 10^{-10}\,\mathrm{m}^2/\mathrm{s}$, $D_{21} = -1.08 \cdot 10^{-10}\,\mathrm{m}^2/\mathrm{s}$, $D_{22} = 11.10 \cdot 10^{-10}\,\mathrm{m}^2/\mathrm{s}$, thermal diffusion coefficients $D_{T1} = -0.81 \cdot 10^{-12}\,\mathrm{m}^2/\mathrm{s\,K}$, $D_{T2} = -0.93 \cdot 10^{-12}\,\mathrm{m}^2/\mathrm{s\,K}$ and separation ratios $\psi_1 = 0.324$ and $\psi_2 = 0.126$ [26]. The transformation (6) gives $\hat{\psi}_1 = 0.109$, $\hat{\psi}_2 = 0.341$ and $\hat{\mathrm{Sc}}_1 = 1390$, $\hat{\mathrm{Sc}}_2 = 2244$. The positive values of separation ratios show that the instability is possible only for heating from below. Linear and nonlinear calculations performed at this type of heating confirm the onset of monotonic instability at the Rayleigh number $\mathrm{Ra_c} \approx 27.2$. The temporal evolution flow characteristic repeats qualitatively the results obtained for the model mixture (figs. 3, 4). Fields of the stream function and concentration for Ra = 40 are shown in fig. 13 (the concentration fields obtained in the calculations based on eqs. (7)–(12) were subjected to the inverse transformation (6)). For this mixture the diagonalization procedure has not brought qualitative changes as compared to the results of the calculations.

7 Conclusion

The paper presents the results of a numerical investigation of the linear stability of mechanical equilibrium and nonlinear convection regimes of ternary mixtures in a square cavity with rigid, impermeable boundaries subjected to the gravity field and vertical temperature gradient. The dependences of critical parameters on net separation ratio of the mixtures are determined. The boundaries of monotonic and oscillatory instabilities for heating from below and the boundary of monotonic instability for heating from above, as well as the structure of the stream function, temperature and concentration fields are obtained. Numerical data on the structure of nonlinear regimes for the model ternary mixtures with different values of net separation ratios, giving different types of instabilities, are obtained. For hydrocarbon mixture dodecane-isobutylbenzene-tetralin the data on nonlinear flow regime at heating from below are obtained and compared with the results obtained for the model mixture.

The work was supported by Russian Scientific Foundation (grant No. 14-01-00090).

References

1. G.Z. Gershuni, E.M. Zhukhovitskii, *Convective Stability of Incompressible Fluid* (Israel Program for Scientific Translations, Jerusalem, 1976).
2. M. Lücke, W. Barten, P. Büchel, C. Fütterer, St. Hollenger, Ch. Jung, Lect. Notes Phys. **55**, 127 (1998).
3. V.M. Shevtsova, D.E. Melnikov, J.C. Legros, Phys. Rev. E **73**, 047302 (2006).
4. M.C. Kim, C.K. Choi, J.-K. Yeo, Phys. Fluids. **19**, 084103 (2007).
5. M.I. Shliomis, M. Souhar, Europhys. Lett. **49**, 55 (2000).
6. R. Cerbino, A. Vailati, M. Giglio, Phys. Rev. E **66**, 055301(R) (2002).
7. S. Mazzonia, R. Cerbino, D. Brogioli, A. Vailati, M. Giglio, Eur. Phys. J. E **15**, 305 (2004).
8. R. Cerbino, S. Mazzoni, A. Vailati, M. Giglio, Phys. Rev. Lett. **94**, 064501 (2005).
9. F. Croccolo, F. Scheffold, A. Vailati, Phys. Rev. Lett. **111**, 014502 (2013).
10. M. Italia, F. Croccolo, F. Scheffold, A. Vailati, Eur. Phys. J. E **37**, 101 (2014).
11. I.I. Ryzhkov, *Thermal Diffusion in Mixtures: Equations, Symmetries and Solutions and their Stability* (Institute of Computational Modelling SB RAS, Krasnoyarsk, 2012) p. 215.
12. S.M. Cox, I.M. Moroz, Physica D **93**, 1 (1996).
13. J.P. Larre, J.K. Platten, G. Chavepeyer, Int. J. Heat Mass Transfer **40**, 545 (1997).
14. A. Mialdun, V.M. Shevtsova, Int. J. Heat Mass Transfer **51**, 3164 (2008).
15. A. Leahy-Dios, A. Firoozabadi, J. Phys. Chem. B **111**, 191 (2007).
16. M.C. Charrier-Mojtabi, B. Elhajjar, A. Mojtabi, Phys. Fluids **19**, 124104 (2007).
17. A. Vailati, M. Giglio, Phys. Rev. E **58**, 4361 (1998).
18. K. Jamshidi-Ghaleh, M.T. Tavassoly, N. Mansour, J. Phys. D: Appl. Phys. **37**, 1993 (2004).
19. A. Firoozabadi, K. Ghorayeb, SPE J. **5**, 158 (2000).
20. T. Lyubimova, N. Zubova, Micrograv. Sci. Technol. **26**, 241 (2014).
21. I.I. Ryzhkov, V.M. Shevtsova, Phys. Fluids **21**, 014102 (2009).
22. A.Yu. Gelfgat, J. Comput. Phys. **156**, 300 (1999).
23. D.V. Lyubimov, T.P. Lyubimova, V.A. Morozov, Bull. Perm Univ. Info. Syst. Technol. **5**, 74 (2001).
24. E.T. Whittaker, G. Robinson, *The Newton-Raphson Method*, Ch.44 in *The Calculus of Observations: A Treatise on Numerical Mathematics*, 4th edition (Dover, New York, 1967) pp. 84–87.
25. A. Thom, C.J. Apelt, *Field Computations in Engineering and Physics* (Van Nostrand, London, 1961).
26. P. Blanco, M.M. Bou Ali, J.K. Platten, D.A. Nezquia, J.A. Madariaga, C. Santamaria, J. Chem. Phys. **132**, 114506 (2010).